Author's personal copy

Journal of Atmospheric and Solar-Terrestrial Physics 77 (2012) 85–95

Contents lists available at SciVerse ScienceDirect

Journal of Atmospheric and Solar-Terrestrial Physics

journal homepage: www.elsevier.com/locate/jastp

Determination of the wave mode contribution into the ULF pulsations from combined radar and magnetometer data: Method of apparent impedance

V. Pilipenko [a,*], V. Belakhovsky [b], A. Kozlovsky [c], E. Fedorov [a], K. Kauristie [d]

[a] Institute of the Physics of the Earth, Moscow, Russia
[b] Polar Geophysical Institute, Apatity, Russia
[c] Sodankyla Geophysical Observatory of the Oulu University, Finland
[d] Finnish Meteorological Institute, Helsinki, Finland

ARTICLE INFO

Article history:
Received 7 July 2011
Received in revised form
20 November 2011
Accepted 28 November 2011
Available online 7 December 2011

Keywords:
MHD waves
ULF pulsations
Ionosphere
Radar
Magnetometer
Acoustic-gravity waves

ABSTRACT

To identify the physical nature of Pc5 pulsations and to determine relative contributions of different MHD modes into their structure, we introduce the method of apparent impedance. An approximate analytical relationship from the theory of ULF wave transmission through a thin ionosphere can be compared with the measured ratio between simultaneous ionospheric electric and ground magnetic fields. The analytical expressions show that the impedances of Alfven and compressional modes should be essentially different. To validate this technique, we have analyzed global *Pc*5 pulsations during the recovery phase of the strong magnetic storm on October 31, 2003 using ground magnetometricdata and tri-static EISCAT radar. This radar facility gives a possibility to calculate vectors of the F-region ionospheric plasma flow and electric field. From these observations we conclude that the global *Pc*5 pulsations during storm conditions above the ionosphere are predominantly composed from Alfven waves with a small contribution of fast compressional mode.

© 2011 Elsevier Ltd. All rights reserved.

1. Introduction

The near-Earth space is filled with various long-period ULF modes. Some examples addressed in literature are large-scale toroidal (Fenrich et al., 2006) and small-scale poloidal (Yeoman et al., 2000) Alfven waves, compressional oscillations (Kivelson et al., 1984), and slow ion-sound mode waves (Leonovich et al., 2006). Satellite observations have shown that many types of ULF waves, e.g. storm-time Pc5 (Pokhotelov et al., 1985), Pi2 (Sutcliffe and Luhr, 2005), and Pc3 (Pilipenko et al., 2011) pulsations have a substantial compressional component and cannot be interpreted as a pure Alfven shear wave. Moreover, there are theoretical indications on the possibility of coupled Alfven and trapped magnetosonic modes in the magnetosphere, corresponding to oscillations of either the magnetospheric cavity mode (Leonovich and Mazur, 2005; Samson et al., 1991), or the magnetospheric waveguide (Mann et al., 1999). The evanescent fast compressional mode emerges upon the interaction of Alfven waves with the anisotropic ionosphere, which has been confirmed by Doppler sounding (Sutcliffe and Poole, 1990; Alperovich et al., 1991). Thus, magnetospheric Pc5 pulsations are in general a complicated mixture of Alfven and magnetosonic waves. So far, the only technique to discriminate the different ULF modes has been the comparisons of transverse and field-aligned (compressional) magnetic components during occasional satellite observations.

Various high time-space resolution radars, such as SABER, STARE, SuperDARN, and EISCAT have become a widely used tool to detect ULF wave interaction with the ionosphere, where these waves transfer energy through the coupled magnetosphere–ionosphere system. Radar data are commonly used in ULF studies to characterize the global ionospheric electrodynamical context of the analyzed ULF event and to identify the ionospheric projection of magnetospheric domains (Clauer et al., 1997) in the surroundings of the event. The ULF activity in the ionosphere detected by radars has been interpreted as signatures of Alfven wave incidence onto the ionosphere (e.g., Pc5 pulsations (Walker et al., 1979)) or they have been associated with plasmaspheric cavity modes (e.g., Pi2 pulsations (Ikeda et al., 2010)). A statistical study investigating Pc5 pulsation with the use of the SABER VHF coherent radar was reported by Yeoman et al. (1990). The ratio of the pulsation radar backscatter intensity modulations to the ionospheric irregularity drift velocity modulations was used as a tool to determine the wave mode in the radar field of view. In this study the relative impact of compressional Pc5 waves was observed to increase as the azimuthal wave number increased in the range $m=1$–10. Thus, these radar observations of Pc5 pulsations also suggested that compressional modes can contribute to the ULF wave structure. Apart from MHD waves,

* Coresponding author. Tel.: +7 495 4383985.
E-mail address: space.soliton@gmail.com (V. Pilipenko).

1364-6826/$ - see front matter © 2011 Elsevier Ltd. All rights reserved.
doi:10.1016/j.jastp.2011.11.013

Author's personal copy

infrasonic waves with periods in the same Pc5 range (2–5 min) can cause the periodic modulation of the ionospheric plasma and currents (Georges, 1973).

In this paper we present a possibility to use combined radar and magnetometer observations for the ULF mode identification at the ionospheric end. We demonstrate this method to determine the relative contributions of Alfven and fast compressional modes using combined EISCAT radar and magnetometer observations of global Pc5 pulsations. We analyze Pc5 pulsations, which exceed in their amplitude the ordinary Pc5 pulsations by an order of magnitude and which are typically observed during the recovery phase of strong magnetic storms (Kleimenova and Kozyreva, 2005). These oscillations have been observed in the morning and evening sectors simultaneously in a wide latitude range (Potapov et al., 2006). However, the exact wave processes behind these pulsations are still unknown: Are they due to field line Alfven oscillations like ordinary Pc5 pulsations or are they driven by a combination of different wave processes?

2. The method of apparent impedance

2.1. The concept of apparent impedance

As an additional discrimination tool of the different ULF wave modes the measurements of their apparent impedance, i.e., the E/B ratio, can be used. The impedance technique is widely used in satellite observations to identify the nature of electromagnetic structures in space (Knudsen et al., 1992). However, the situation with disturbances in the upper ionosphere is more difficult for this type of analysis. The detected wave fields are composed from a mixture of incident, reflected, and converted modes. Moreover, the ULF magnetic disturbance in the ionosphere cannot be directly measured, and thus it has to be related with the magnetic variations measured at the ground surface. Thus, reasonable identification of the wave mode is possible only on the basis of an adequate theory. Such analytical theory, describing the interaction of long-period ULF wave harmonics with the thin ionosphere, has been developed in numerous papers and summarized in a book by Alperovich and Fedorov (2007). The application of this theory to the study of specific ULF waves' interaction with the realistic ionosphere was made in (Pilipenko et al., 2008). To illustrate here the basic idea of the apparent impedance method, some approximate relationships derived from the above mentioned papers are given.

The idea of this approach is as follows. The radar (e.g. EISCAT) observations of ULF waves in the upper ionosphere can detect oscillations of the ionospheric plasma with velocity $\mathbf{V}=[\mathbf{E}\times\mathbf{B}_0]/B_0^2$, induced by a wave electric field $\mathbf{E}$ in the geomagnetic field $\mathbf{B}_0$. From $\mathbf{V}$ data the corresponding wave $\mathbf{E}$-field can be obtained as $\mathbf{E}=[\mathbf{V}\times\mathbf{B}_0]$. In the region where EISCAT measures (high latitudes) $\mathbf{B}_0$ is roughly in vertical direction and $B_0\sim 5\cdot 10^4$ nT. In such conditions as an order of magnitude estimate the relationship between V and E can be expressed as $V[\mathrm{m/s}]=20\ E[\mathrm{mV/m}]$. Simultaneously with the radar observations the ground magnetometers measure the wave magnetic component $\mathbf{B}^{(g)}$. The combination of the electric and magnetic field data provides the ratio which we name the apparent spectral impedance of the ionospheric wave structure

$$Z_{xy}(\omega)=\mu_0\frac{E_x(\omega)}{B_y(\omega)},\quad Z_{yx}(\omega)=\mu_0\frac{E_y(\omega)}{B_x(\omega)},\ldots$$

where magnetic constant $\mu_o=4\pi\times 10^{-7}$H/m. The intrinsic wave impedance characterizes the properties of a medium to a particular wave. For example, for an Alfven wave propagating in a homogeneous medium with the Alfven velocity V_A and wave conductance $\Sigma_A=1/\mu_0 V_A$, the impedance is to be $Z_{xy}=-Z_{yx}=Z_A=\Sigma_A^{-1}$. For an electromagnetic wave propagating in free space the impedance is $Z_o=\sqrt{\mu_o/\varepsilon_o}$. For a multi-layer medium, an impedance is determined by the property of a layer, where a wave will propagate.

For a practical application we suggest to use the ratio $E/B=Z/\mu_o$, named the impedance velocity, having the dimension of velocity, namely

$$U_{xx}(\omega)=\frac{E_x(\omega)}{B_x^{(g)}(\omega)},\quad U_{yx}(\omega)=\frac{E_y(\omega)}{B_x^{(g)}(\omega)},\ldots$$

In convenient units, the additional numeric factor should be taken into account, namely $U[\mathrm{km/s}]=10^3 E[\mathrm{mV/m}]/B[\mathrm{nT}]$. This impedance velocity U_{ij} has to be compared with the theoretically predicted medium parameters.

2.2. Alfven mode incidence with the ionosphere

We use a coordinate system where the X-coordinate corresponds to the Southward (radial) direction, Y corresponds to the Eastward (azimuthal) direction, and Z is vertical up in the Northern hemisphere. In a large-scale toroidal Alfven mode (the azimuthal wave number $m\sim 1$) the dominant components are B_y, E_x, V_y, and no magnetic field compression $B_\parallel$. This mode is excited by MHD disturbances from the distant magnetosphere via the field line Alfven resonance. In a small-scale poloidal mode ($m\gg 1$) the dominant components are B_x, E_y, and V_x. This mode is excited by magnetospheric energetic particles. In the transmission of an Alfvenic mode through the ionosphere the wave ellipse rotation should occur $B_y\to B_x^{(g)}$ ($B_x^{(g)}=-H$ component), $B_x\to B_y^{(g)}$ ($B_y^{(g)}=D$ component).

The ground magnetic response to the azimuthally small-scale Alfven waves is controlled by the factor $\exp(-k_y h)$, where k_y is the local azimuthal component of the wave vector in the ionosphere at the geomagnetic shell L, and h is the height of the ionospheric E-layer (Hughes and Southwood, 1976). The critical m-value, when $k_y h=1$, is $m^*=(R_E/h)L^{-1/2}$, which for $L=6.6$ yields $m^*\sim 20$. Therefore, waves with $m<m^*$ produce magnetic response on the ground, whereas waves with $m\gg m^*$ are screened by the ionosphere. Hereafter we assume that the waves under consideration are azimuthally large-scale, i.e. $m<m^*$.

The interaction of long-wavelength ULF waves with the coupled magnetosphere–ionosphere–atmosphere–ground system can be considered under the thin ionosphere approximation. This approximation assumes that the wave skin-depth δ_P, which is determined by the E-layer Pedersen conductivity σ_P, namely $\delta_P=\sqrt{2/(\mu_0\omega\sigma_P)}$, is larger than the thickness of the ionospheric conductive layer Δh. For Pc5 waves in the dayside ionosphere δ_P is 1–2 orders of magnitudes larger than the typical $\Delta h\sim 20$ km. In addition, in the case of compressional mode incidence the horizontall wavelength of the wave is typically much larger than the conductive ionospheric layer thickness, $k_x\Delta h\ll 1$. Thus, for the event analyzed later in this paper the thin ionosphere approximation is well satisfied. The finite-width effects, neglected here, may cause an additional polarization change and ellipticity upon the transmission of fast compressional mode through the E-layer (Nenovski, 2001). However, for the considered Pc5 event $(k_x\delta_P)^2\sim 10$, and $\Sigma_H/\Sigma_P\sim 1$–2, this effect is about 2° only according to (Nenovski, 2001) calculations.

Upon the reflection of the incident Alfven wave with intermediate transverse scales from the ionosphere the inductive part of the wave electric field commonly can be neglected (Yoshikawa and Itonaga, 1996; Yagova et al., 1999). However, for a high-frequency wave (e.g. Pc2–3) incident on the highly-conductive ionosphere an additional inductive shielding of an incident signal

Author's personal copy

from ground magnetometers can occur (Yoshikawa et al., 2002). This shielding is caused by the conversion of a part of the Alfven wave energy into the surface-type ionospheric gyrotropic mode (Pilipenko et al., 2000). The extension of the proposed approach to this case would demand the use of more complicated relationships, accounting for inductive effects and finite ground conductivity (for more information, see the above cited papers).

As a consequence of the interaction of an Alfven wave with the anisotropically-conductive ionosphere a fast compressional mode is excited (Hughes and Southwood, 1976). This mode has an evanescent vertical structure, decaying with altitude z as $\propto \exp(-kz)$. Its excitation rate is characterized by the scale-dependent reflection coefficient $R_{FA}(k)$ (Alperovich and Fedorov, 2007). The excitation of this mode becomes noticeable only for rather small transverse scales, $k \geq 10^{-3}\mathrm{km}^{-1}$, and its amplitude becomes comparable to the incident wave amplitude at $k \sim 10^{-2}\mathrm{km}^{-1}$. Therefore, the contribution of the fast mode into the ULF wave structure in the F-layer ($z \sim 200$ km) is 10% less for the wave transverse scale $L < 2\pi/k \sim 570$ km. For a larger scale wave the decay of its amplitude with altitude is not so dramatic, but its excitation rate $\sim R_{FA}(k)$ is low. Though this mode can noticeably modulate the plasma of F-layer and total electron content (TEC) (Poole and Sutcliffe, 1987; Pilipenko and Fedorov, 1995), it does not contribute to the dominant Alfven component E_x recorded by a radar.

From the general theory of the large-scale ($k_y \to 0$) Alfven wave transmission through the thin ionosphere to the ground it follows that the wave spatial spectrum near the ground $B_x^{(g)}(k_x)$ is related to the spatial harmonic of magnetic disturbance in the ionosphere $B_y(k_x)$ by the well-known relationship (Nishida, 1964; Hughes and Southwood, 1976)

$$B_x^{(g)}(k_x) = -B_y(k_x)\frac{\Sigma_H}{\Sigma_P}\sin I \exp(-k_x h) \tag{1}$$

where I is the magnetic field inclination ($I > 0$ in the Northern hemisphere). The relationship (1) predicts that only waves with small and intermediate m values, up to ~ 20, can be detected on the ground, whereas poloidal Alfven waves with large $m \gg 20$ are screened by the ionosphere from ground magnetometers and cannot be examined with the proposed impedance technique. If a localized Alfvenic structure in the magnetosphere has been produced by the resonant conversion (like e.g. in the case of Pc5 with field line resonance characteristics), its radial structure can be reasonably well modeled as:

$$B_y(x) = B^{(m)}\frac{i\delta_m}{x - x_o + i\delta_m}$$

Here δ_m is the width of the resonant structure above the ionosphere, and $B^{(m)}$ is the peak value of resonant structure. The spatial structure of magnetic disturbance near the ground $B_x^{(g)}(x)$ is found by the inverse Fourier transform of the spatial spectrum of the above magnetospheric structure multiplied by the transmission factor (1)

$$B_x^{(g)}(x) = -B^{(m)}\frac{\Sigma_H}{\Sigma_P}\sin I\frac{i\delta_m}{x - x_o + i(\delta_m + h)}$$

Thus, the ground magnetic response to the magnetospheric resonant structure has the same spatial form as an incident wave, but peak amplitude at $x \to x_0$ is reduced by the factor $(\Sigma_H/\Sigma_P)\sin I\delta_m/(\delta_m + h)$, and peak width is smeared $(\delta_m + h)\delta_m$ times. If the Alfvenic structure is not very narrow, $\delta_m > h$, the relationship between the maximal ionospheric magnetic disturbance and its ground response is $B_x^{(g)} \sim B_y^{(m)}(\Sigma_H/\Sigma_P)\sin I$.

The impedance of an Alfven wave interacting with the multilayered system magnetosphere–thin ionosphere is determined by the relationship

$$Z(z,\omega) = \Sigma_A^{-1}\frac{\Sigma_A - i\Sigma_P \tan k_A z}{\Sigma_P - i\Sigma_A \tan k_A z}$$

This relation coincides with formula for $Z(\omega)$ from (Knudsen et al., 1992). The measured wave impedance should vary with altitude z in the range from Σ_P^{-1} to Σ_A^{-1}. At low altitudes, $z \ll k_A^{-1}$, the above relationship is reduced to the well-known relation $Z(\omega) = \Sigma_P^{-1}$. Thus, for a azimuthally large-scale Alfven mode, $k_y \ll k_x$, the dominant B_y and E_x components at the ionospheric altitudes less than few thousands km are related as

$$\frac{E_x}{B_y} = -V_P \sin^2 I$$

These components are to be in-antiphase. The characteristic ionospheric velocities $V_{P,H,C} = (\mu_o \Sigma_{P,H,C})^{-1}$ are determined by the height-integrated Pedersen Σ_P, Hall Σ_H, and Cowling $\Sigma_C = \Sigma_P(1 + \Sigma_H^2/\Sigma_P^2)$ ionospheric conductances (Fedorov et al., 1999). For the order of magnitude estimate the following relationship can be used $V[\mathrm{km}/s] \approx 800/\Sigma[S]$.

The experimentally measured impedance-like relationship, using the ground magnetic disturbance $B_x^{(g)}$, for large-scale ($k_x h < 1$, $k_y \to 0$) Alfven mode is to be

$$U_{xx}^{(A)} \equiv \frac{E_x}{B_x^{(g)}} = -\frac{V_H}{\sin I} \tag{2}$$

The non-dominant wave electric component E_y, induced upon the Alfven wave interaction with the ionosphere, is related to ground magnetic component $B_x^{(g)}$ in a large-scale mode $k_x h < 1$ as follows:

$$U_{yx}^{(A)} = \frac{E_y(z)}{B_x^{(g)}} = -i\omega h$$

These components are to be in quadrature ($\pi/2$ phase shift). Thus, for a large-scale Alfvenic mode with $k_y \to 0$ the apparent impedance velocities U_{xx} and U_{yx} are to be different: U_{yx} is about few km/s, that is much less than U_{xx}. However, in realistic situation, the non-dominant component E_y is weak and contaminated by the stronger E_x component, so a lower magnitude of U_{yx} hardly can be revealed.

Hence, wave with $B \sim 100$ nT induces electric field disturbance $E \sim 8$ mV/m in the daytime ionosphere ($\Sigma_H \sim 10$ S), and $E \sim 80$ mV/m during nighttime ($\Sigma_H \sim 1$ S). This value of E produces electric drift with velocity $V \sim$ 160 m/s during daytime, and $V \sim 1.6$ km/s during nighttime.

2.3. Fast mode incidence on the ionosphere

In principle, wave energy can be transported from a magnetospheric source towards the ground by a fast magnetosonic (compressional) mode. Large-scale ($m \to 0$) fast mode has dominant components B_x, E_y, V_x with vanishing field-aligned current $j_\parallel = 0$. Upon the transmission through the ionosphere no rotation occurs, that is $B_x \to B_x^{(g)}$ (H-component), $B_y \to B_y^{(g)}$ (D-component).

The wave scale of the fast mode in the Pc5 range in the magnetosphere is expected to be very large (e.g., $\sim k_A^{-1} \sim 8R_E$ for $T = 300$ s, and $V_A = 10^3$ km/s). Therefore, fast waves cannot reach the ionosphere directly under reasonable horizontal wave numbers, because upon their propagation toward plasma with a higher V_A they encounter a non-propagation (opaque) region, where the field-aligned component of the wave vector fulfills the condition $k_F^2 < 0$. However, because of its large horizontal scale, even an evanescent fast mode can convey significant wave energy towards the Earth.

The ratio of the ground magnetic signal $B_x^{(g)}$ to the incident compressional wave amplitude B_x is determined by the transmission

Author's personal copy

properties of the whole ionosphere–atmosphere–ground system. For the highly-conductive ground ($\sigma_g \to \infty$), the relationship between the magnetic disturbance in the ionosphere and its ground response is

$$\frac{B_x}{B_x^{(g)}} = 1 - ip, \quad p = \frac{\omega h}{V_C}$$

The parameter p controls the penetration of the fast mode through the ionosphere. If $|p| \ll 1$ (e.g., at nightside) the ionosphere may be considered to be transparent for the fast mode, so the incident wave is reflected mainly by Earth's surface. Upon this reflection, magnetic disturbance near the ground doubles as compared with amplitude of incident wave. If $|p| \sim 1$ (e.g., at dayside) the ionosphere partially screens the magnetospheric signal from the ground.

At low altitudes above the nearly-transparent ionosphere, where $|k_F z| \ll 1$, the dominant electric component of the fast mode E_y is related to the magnetic ground response $B_x^{(g)}$ by the following impedance-like relationship:

$$U_{yx}^{(F)} = \frac{E_y(z)}{B_x^{(g)}} = -i\omega(z+h) \tag{3}$$

The fast mode electric field is to be in quadrature ($\pi/2$ phase shift) to magnetic field variations on the ground.

In general, the electric field induced in the ionosphere by a fast mode is weaker than that by an Alfven mode for the same magnitude of the ground magnetic signal. Indeed, comparison of (2) and (3) shows that

$$\left|\frac{U^{(F)}}{U^{(A)}}\right| = \frac{\omega(z+h)\sin I}{V_H}$$

For dayside Pc5 wave $\omega = 0.01\ \mathrm{s}^{-1}$, $z+h = 300$ km, and $V_H = 80$ km/s this ratio is ~ 0.04. Thus, for typical Pc5 parameters

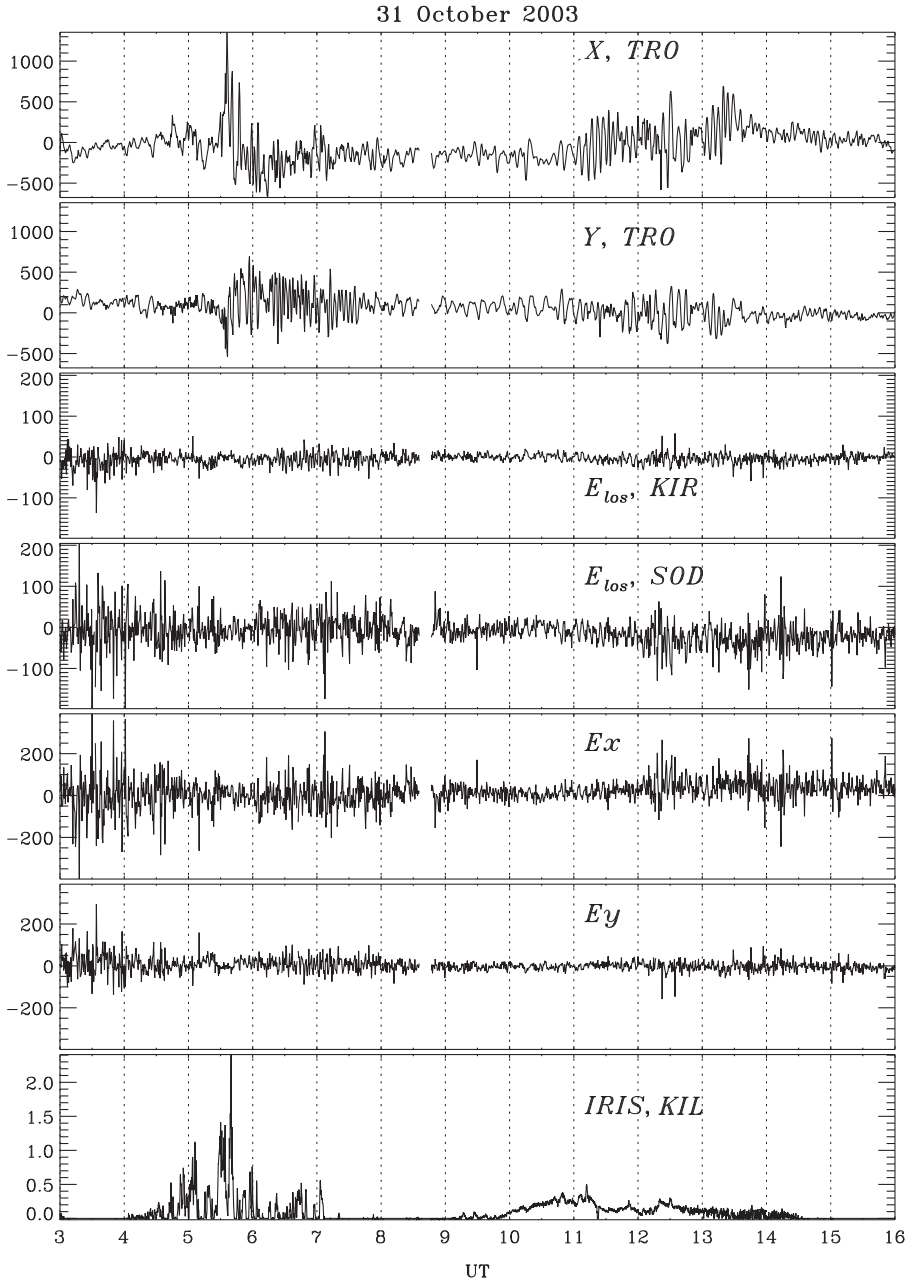

Fig. 1. Variations of geomagnetic field at TRO X and Y components (in nT), ionospheric line-of-sight electric field along the beam from KIR and SOD (in mV/m), components E_x and E_y of the ionospheric electric field (in mV/m), and riometer absorption measured at KIL during October 31, 2003 03–16 UT.

Author's personal copy

the amplitude of the impedance velocity of fast compressional modes is essentially less than that of Alfven modes.

Though, because Alfven mode and fast mode are polarized in a different manner, their impact on the ionospheric plasma may be comparable. For example, the dominant toroidal Alfvenic component E_x does not produce any vertical drift of the ionospheric plasma, whereas the dominant fast mode component E_y does ($V_z = E_y \cos I/B_0$). As a result, during the Doppler measurements the effect of fast mode can even prevail that of the Alfven mode (Sutcliffe and Poole, 1990; Alperovich et al., 1991).

2.4. Atmospheric waves

The magnetic field disturbance, induced by atmospheric waves (e.g. acoustic or internal gravity) in a conductive ionosphere can be estimated (Pogorel'zev, 1989) as follows:

$$\frac{B}{B_0} \sim \mu_o \sigma_P u \Delta z \tag{4}$$

Here u is the disturbed velocity of the neutral gas, Δz is the thickness of the interaction region, σ_P is the typical value of Pedersen conductivity. If the interaction region comprises the conductive E-layer, ionospheric currents induced by an atmospheric wave produce a measurable ground magnetic response. The transverse scale of acoustic wave in the Pc5-6 frequency band is large as compared with the height of E-layer, so the ground magnetic response is to be about the same as magnetic disturbance in the ionosphere (4).

The electric field disturbance, induced by atmospheric wave, is $E \sim V_S.B$, where V_S is the atmospheric wave phase velocity (Pogorel'zev, 1989). Therefore, the apparent impedance velocity of electromagnetic disturbance produced by the neutral gas oscillations is to be

$$U_S = V_S$$

Typical values of acoustic velocity V_S in the ionosphere is $\sim$1 km/s. Therefore, the apparent impedance of acoustic-related electromagnetic disturbance is to be much less than that produced by magnetospheric MHD wave. This feature can be used to discriminate ionospheric disturbances produced by acoustic wave and MHD mode.

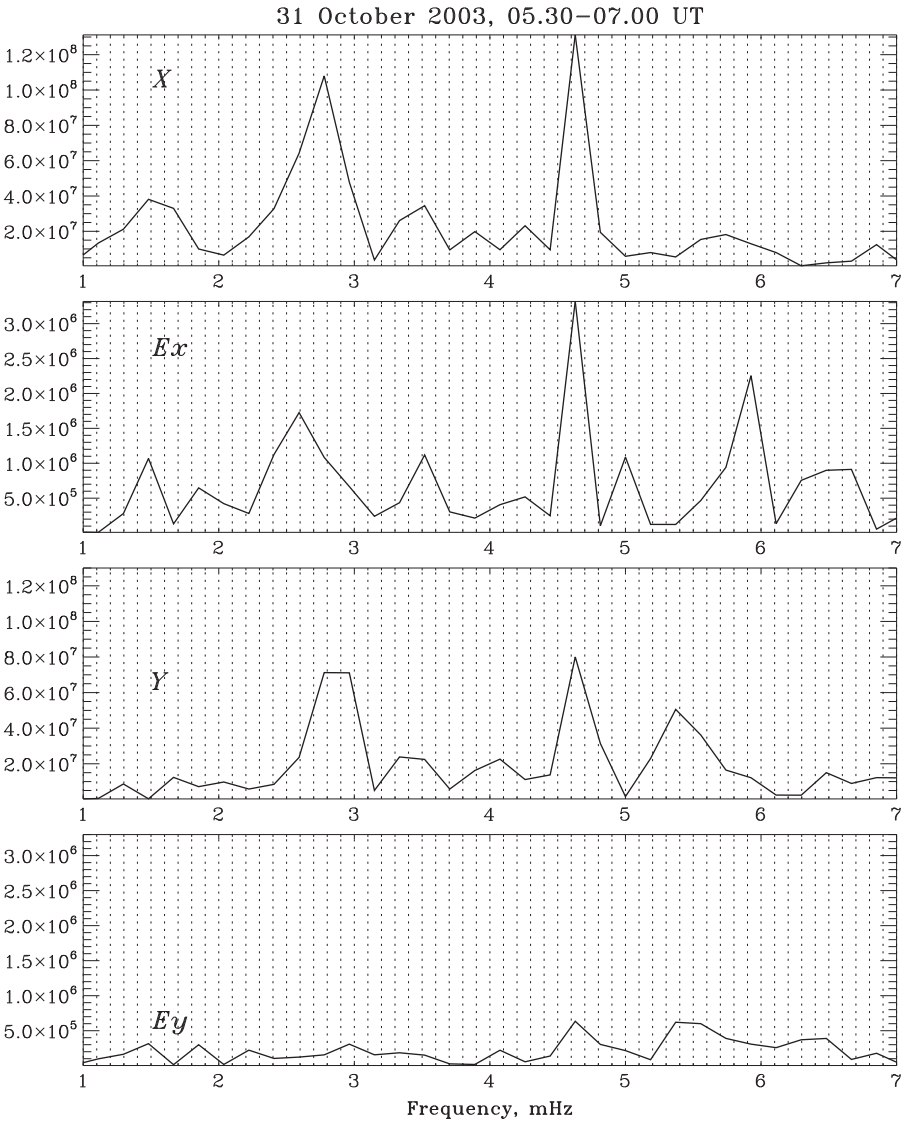

Fig. 2. Spectra during the early-morning interval (0530–0700 UT): variations of magnetic X-component (in nT), electric E_x-component (in mV/m), magnetic Y-component (in nT), and electric E_y-component (in mV/m).

Author's personal copy

2.5. Impedance of coupled MHD mode

Let us suppose that ULF field is composed from contributions of both Alfven and fast modes. In the idealistic case $m \to 0$, we have $E_x = E_x^{(A)}$, $E_y = E_y^{(F)}$, and $B_x = B_x^{(A)} + B_x^{(F)}$. Let us suppose that a relative contribution of fast mode into the ULF wave field is $\delta = B_x^{(F)}/(B_x^{(A)} + B_x^{(F)})$. Then the apparent impedance of the coupled mode is as follows:

$$U_{xx} = U_{xx}^{(A)}(1-\delta) \tag{5}$$

Because for Pc5 waves $U_{xx}^{(A)} \gg U_{yx}^{(F)}$ and $\delta < 1$, so $U_{yx} = U_{yx}^{(F)} \delta U_{xx}$. Therefore, as follows from (5) the apparent impedance of coupled Alfven and magnetosonic mode is to be less than Alfvenic impedance. The deviation between the Alfvenic impedance velocity $U_{xx}^{(A)}$ and the apparent impedance velocity U_{xx} may characterize the relative contribution δ of fast mode.

2.6. Technique validation: the global Pc5 event on October 31, 2003

For validation of the proposed method, we use the EISCAT radar 30-s data from the tri-static Tromso–Kiruna–Sodankylä system, which allows calculating the vectors of the F-region ionospheric plasma flow **V** and electric field **E**. The radar data are analyzed together with IMAGE magnetometer 10-s data from

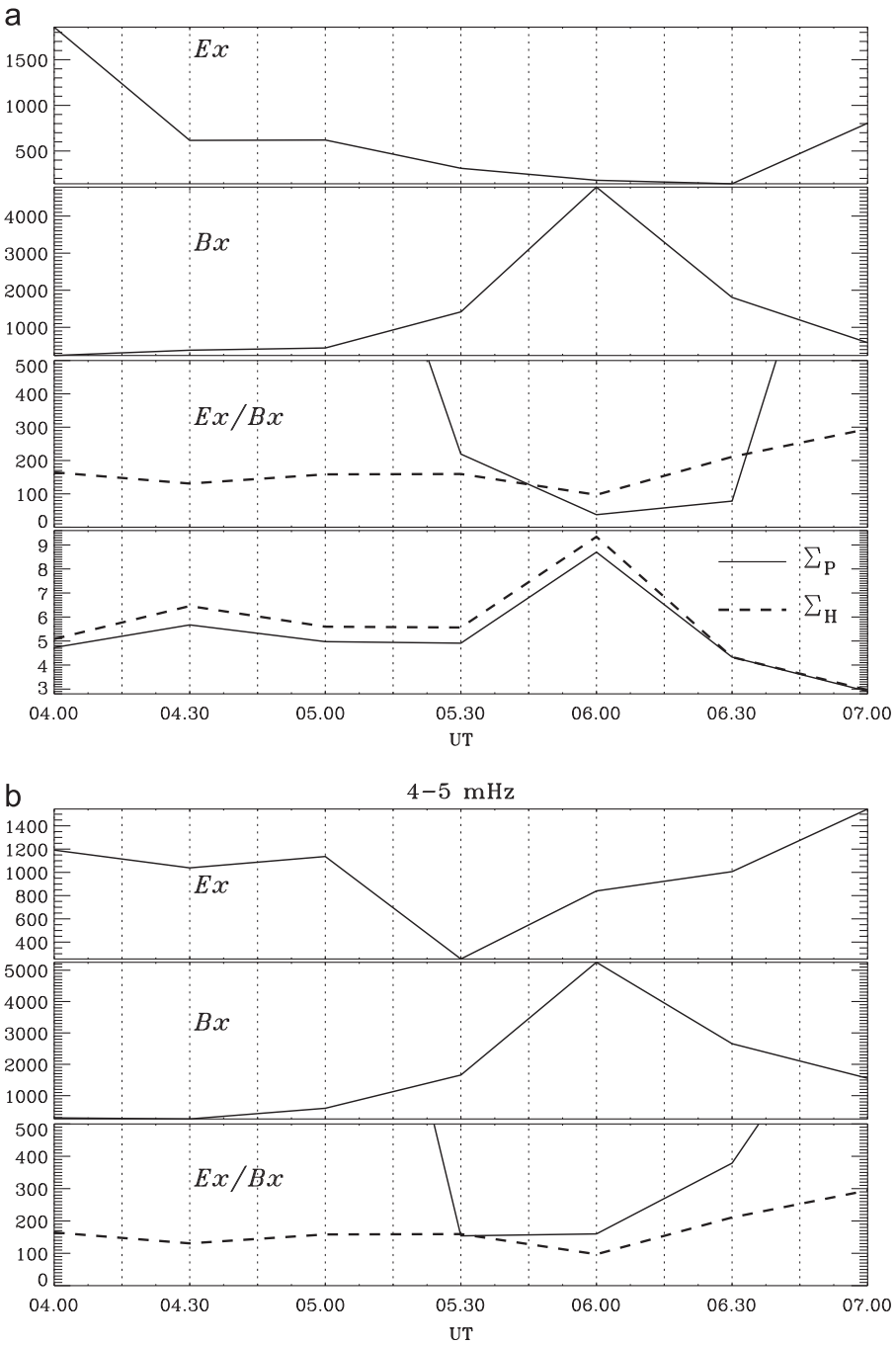

Fig. 3. Spectral powers of $E_x(t)$ and $B_x(t)$ variations, impedance velocities (in km/s) for the time interval 04–07 UT estimated in a running 30-min window from the power spectral densities (solid line) and theoretically predicted for Alfven wave (dashed line) in the band 2.5–3.2 mHz (upper panels), and in the band 4.0–5.0 mHz (bottom panels).

Author's personal copy

the near-by station Tromso. We consider the event on October 31, 2003 when global *Pc*5 pulsations were observed in the morning and afternoon MLT sectors (Kleimenova and Kozyreva, 2005; Belakhovsky and Pilipenko, 2010).

We estimate the relative contributions of the fast and Alfven modes into the ULF field in the following way: The apparent impedance velocity (that is, ratio E_x/B_x) has been estimated from the measured $E(t)$ and $B(t)$ values. Then, using the ionospheric conductivity values deduced from the radar data, the ionospheric velocities $V_P(t)$ and $V_H(t)$ have been calculated via Σ_P, Σ_H. For a pure Alfven mode, these two parameters should match with the relation (2). Deviations from this relation can be related with the contribution of a fast compressional mode ($\sim\delta$). We have applied two approaches to estimate the apparent impedance:

- Amplitudes and phases of both the ionospheric electric, $E(t)$ and $\phi_E(t)$, and ground magnetic, $B(t)$ and $\phi_B(t)$, signals have been calculated using the analytical signal representation, based on the Hilbert transform. Then the ratio $U(t)=E(t)/B(t)$ and phase difference $\phi(t)=\phi_E(t)-\phi_B(t)$ have been calculated. Both signals were preliminary band-filtered. The ionospheric conductance sometimes was found to be strongly modulated by Pc5 pulsations. These oscillations were smoothed.
- Ratio between the spectral power densities $E(f)$ and $B(f)$ at the same frequency in a running 30-min window has been estimated.

During analyzed event, Pc5 pulsations at IMAGE array demonstrated two enhancements, early morning 0530–0800 UT and near-noon 1000–1400 UT (Fig. 1). These two intervals will be considered separately.

During the 1st interval of Pc5 activity, 05–07 UT, the electric field E_x fluctuations exhibit several enhancements. Magnetic fluctuations were most evident from ~0530 UT to ~0630 UT. During the magnetic ULF activity enhancement, the ionospheric conductances increase, more than 2 times, due to the electron precipitation, as evidenced by the riometer observations (Fig. 1). The spectra of ionospheric *E*-field and ground magnetic field oscillations have common peaks around ~2.8 and ~4.7 mHz (Fig. 2). In the subsequent analysis the data were band-filtered in the narrow range $\pm$0.5 mHz, around these frequencies.

The corresponding theoretically predicted values of the impedance velocity $U_{xx}^{(A)}$ varied between 200–100 km/s (Fig. 3). The apparent impedance velocity derived from the combined spectral power densities $E_x(f)$ and $B_x(f)$ at f=2.8 mHz turns out to be very close to the theoretically predicted value $U_{xx}^{(A)}$, but somewhat lower. The ionospheric and magnetic fluctuations were nearly in-phase, as expected from theory. During other time intervals, when magnetic fluctuations are not related to Pc5 pulsations (B_x amplitude is less than 50 nT) the determined magnitude of U_{xx} is much higher that the theoretically estimated. This behavior may indicate that during those time intervals the magnetic fluctuations are not produced by magnetospheric waves. The small difference between the observed U_{xx} and theoretically predicted value $U_{xx}^{(A)}$ for an Alfven wave may be due to the contribution of fast mode in the incident wave structure.

The apparent impedance velocity for the same frequency f=2.8 mHz, but estimated with the analytical signal technique, is shown in Fig. 4a. The theoretically predicted value $U_{xx}^{(A)}$ for Alfven wave is somewhat (~20%) lower. Thus, both techniques of the apparent impedance calculation give consistent results.

For analytical signals at f=4.7 mHz (Fig. 4b) the observed U_{xx} and theoretically predicted value $U_{xx}^{(A)}$ nearly match, so the contribution of fast mode in the incident wave structure at this frequency is insignificant.

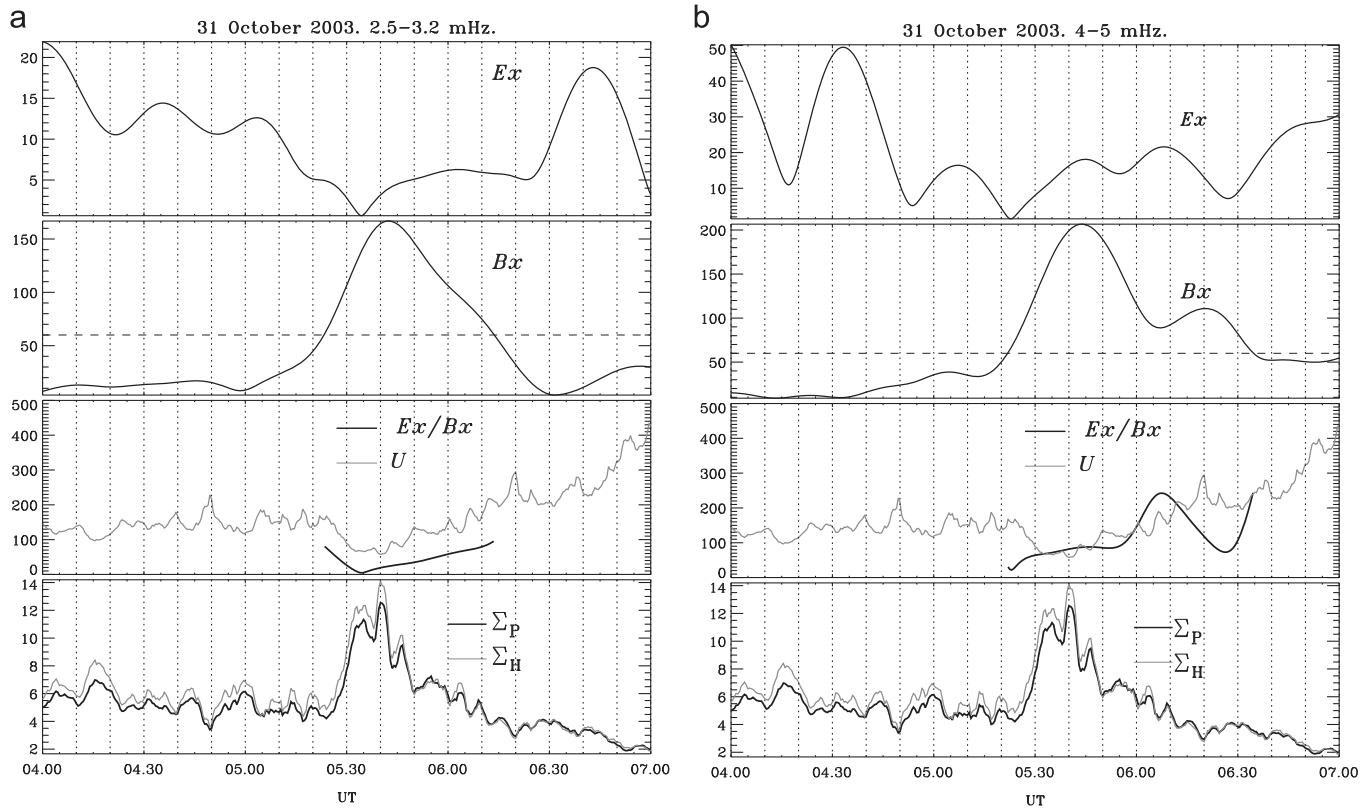

Fig. 4. Amplitudes of $E_x(t)$ and $B_x(t)$ variations, impedance velocities $U_{xx}(t)$ (in km/s) for the 04–07 UT derived from analytical signal (thin line) and theoretically predicted value for Alfven wave (thick line): (a) in the band 2.5–3.2 mHz; (b) in the band 4.0–5.0 mHz. The threshold above noise level is shown by the horizontal dashed line. The bottom panel shows the time variations of ionospheric conductances Σ_P and Σ_H.

Author's personal copy

During the second interval 10–15 UT, the oscillations in the ionosphere and on the ground are concentrated in the spectral band around 3.2 mHz (Fig. 5). Hence, the data have been band-filtered in the range 2.4–4.0 mHz for a further analysis. The ionospheric conductances are nearly the same and gradually vary in the range 4–8 S.

The method using the ratio of spectral powers in a running window is shown in Fig. 6. The same result is confirmed by the analytical signal method. Amplitude envelopes of $E_x(t)$ and $B_x(t)$ variations, estimated with the analytical signal method, demonstrate several enhancements during the period analyzed (Fig. 7). During the time intervals when B_x fluctuations were strong enough (i.e. >100 nT) the calculated impedance velocity U_{xx} was very close to the theoretical value $U_{xx}^{(A)}$ for toroidal Alfven wave. During other time intervals, the calculated value of U_{xx} experiences irregular spikes. The observed magnitude of the apparent impedance velocity turns out to be somewhat lower than $U_{xx}^{(A)}$. This decrease of the impedance velocity is probably caused by a contribution of the compressional mode in the structure of incident Pc5 oscillations.

3. Discussion and conclusion

In this study we provide some additional information on the properties of the global Pc5 pulsations using the simultaneous observations with ground magnetometers and with the EISCAT radar. The resonant effects, which are commonly considered as an indication on Alfvenic nature of ULF pulsations, only weakly presented in the latitudinal distribution of these pulsations (Kleimenova and Kozyreva, 2005). Therefore, these global Pc5 pulsations on October 31, 2003 have been suggested to be signatures of a magnetospheric cavity mode. Comparison of the ground pulsations during this event with simultaneously observed magnetic oscillations at the geostationary orbit (Belakhovsky and Pilipenko, 2010) showed that though GOES spacecraft were located in other MLT sector than the IMAGE magnetometers, the global Pc5 pulsations could be seen at GOES-10 and GOES-12. The variations of the geomagnetic field at GOES-10 during the time interval 05–08 UT, when the morning Pc5 pulsations were observed at IMAGE array, had a significant compressional $B_{\|}$ component. The similar observations of the

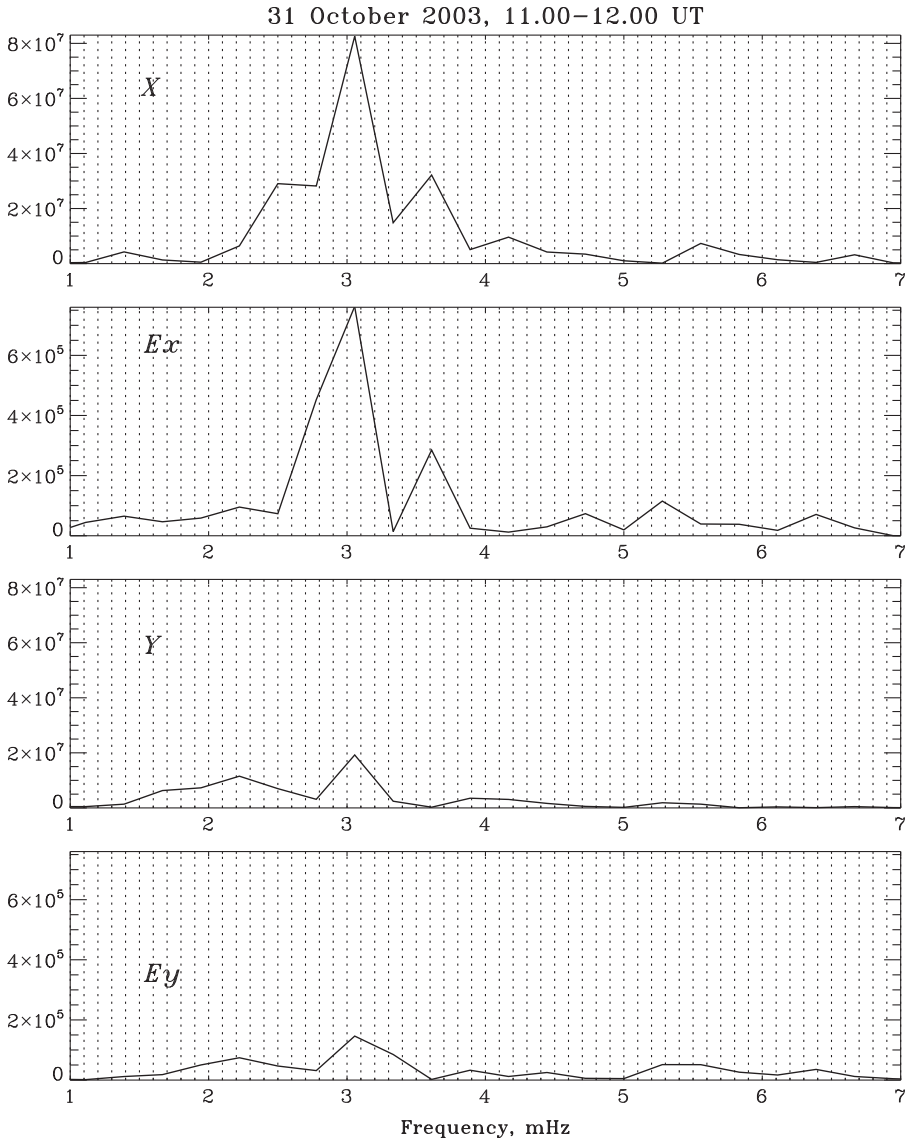

Fig. 5. Spectra of the geomagnetic (X and Y components) and electric (E_x and E_y components) variations during 11–12 UT.

Author's personal copy

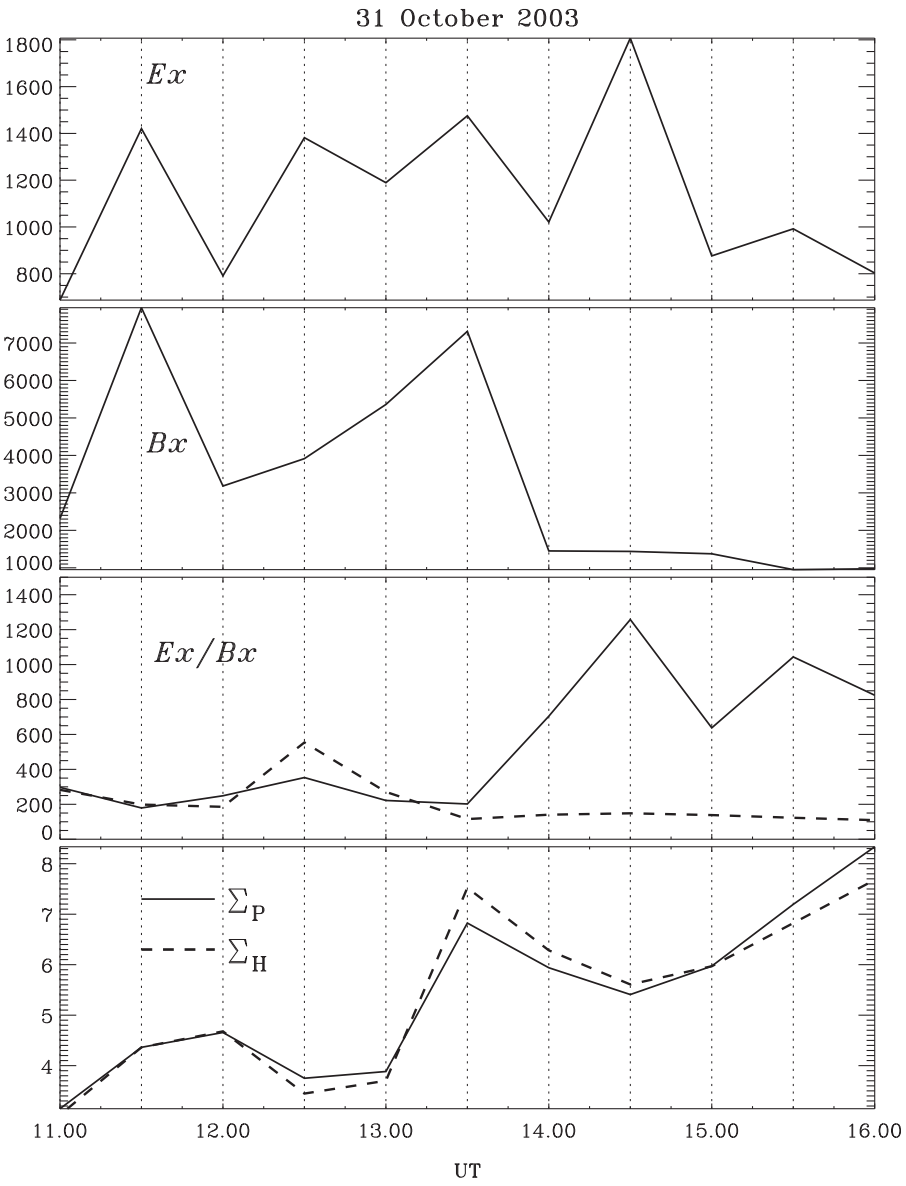

Fig. 6. Spectral powers of $E_x(t)$ and $B_x(t)$ variations, impedance velocities (in km/s) for the time interval 11–16 UT estimated in a running 30-min window from the power spectral densities in the band 2.4–4.0 mHz (thin line) and theoretically predicted for Alfven wave (dashed line).

near-noon Pc5 pulsations at GOES-12 in the interval 10–16 UT also showed that pulsations had a strong compressional component. On the basis of these observations, it was supposed that the global Pc5 pulsations are coupled MHD mode trapped in the magnetospheric waveguide (Pilipenko et al., 2010).

For the analysis of simultaneous radar-magnetometer observations with background ionospheric parameters, the apparent impedance velocity has been introduced to serve as an "easy-to-use" parameter in comparisons. The Alfven wave impedance is to be determined by the ionospheric Hall conductance. At the same time, a fast magnetosonic (or compressional) mode practically does not "feel" the ionosphere, and is reflected mainly from the ground, so its impedance is to be much less than that of the Alfven mode.

The combined ionospheric radar and ground magnetometer observations have shown that the leakage of the compressional mode from the near-equatorial regions of the magnetosphere to the ground is rather small. So, the ULF wave field in the upper ionosphere during the analyzed event is mainly due to the Alfven mode, whereas the contribution of the fast mode has been estimated to be not more than 20%. The apparent contradiction between observations at geostationary satellites and in the upper ionosphere may be explained by assuming that the coupling of Alfven mode with a compressional mode is mainly concentrated in the near-equtorial magnetospheric region, where plasma parameter β reaches a maximal value.

The simple analytical relationships coupling the ratio between the ionospheric signal and its ground response with the ionospheric parameters have been derived in the approximation of negligibly small azimuthal wave number. At very high latitudes, where $I \to \pi/2$, the account of finite k_y reduces to a simple rotation of the coordinate system, such that X-axis is to coincide with the total transverse wave vector $\mathbf{k}_\perp = \{k_x; k_y\}$. However, at lower latitudes, where $I \neq \pi/2$, for a small, but finite k_y, the analytical relationships become too complicated to tackle. Therefore, this case is to be treated numerically. The non-vanishing k_y causes the occurrence of a weak, but noticeable, $B_y^{(g)}$ component.

Author's personal copy

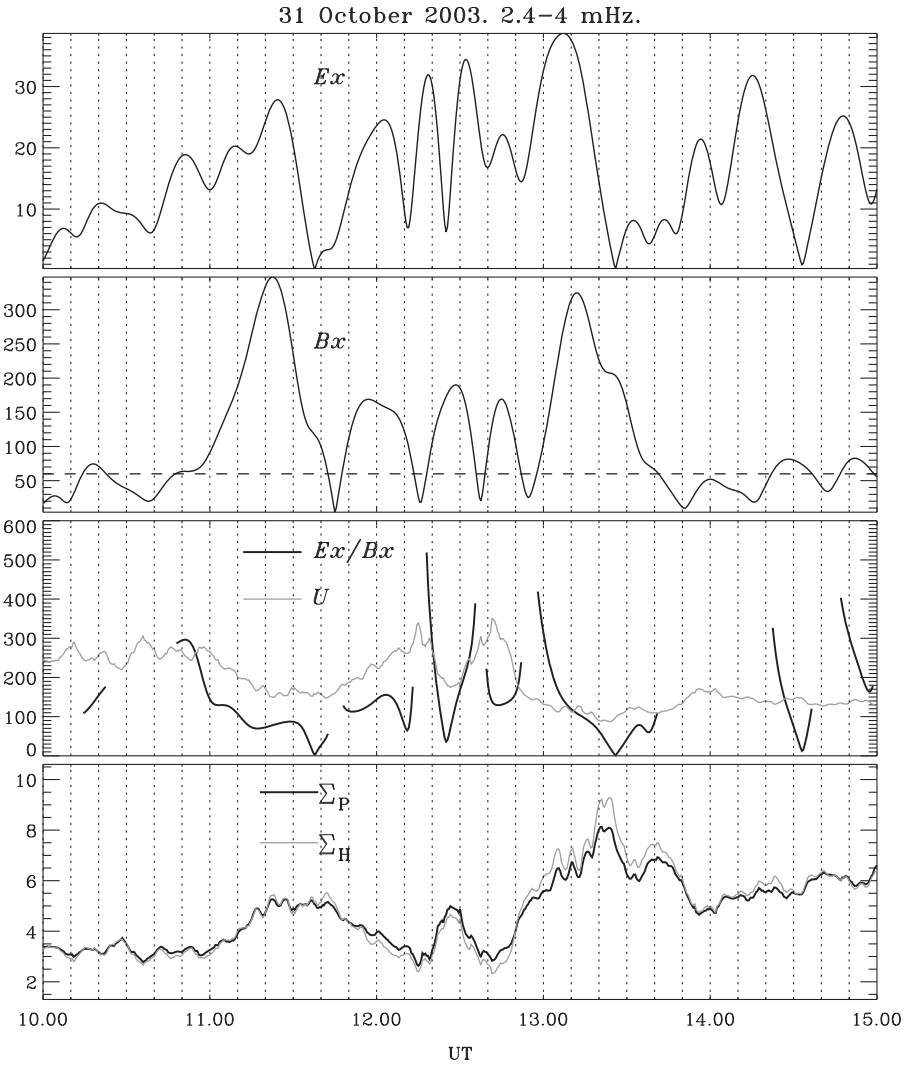

Fig. 7. Amplitudes of $E_x(t)$ and $B_x(t)$ variations, impedance velocities $U_{xx}(t)$ (in km/s) for the 11–16 UT derived from analytical signal in the band 2.4–4.0 mHz (thick line) and theoretically predicted value for Alfven wave (thin line). The threshold above noise level is shown by horizontal dashed line. The bottom panel shows the time variations of ionospheric conductances Σ_P and Σ_H.

Acknowledgments

We are indebted to the Director and staff of EISCAT for operating the facility and supplying the data. EISCAT is an international association supported by research organizations in China (CRIRP), Finland (SA), France (CNRS), Germany (DFG), Japan (NIPR, STEL), Norway (NFR), Sweden (VR), and UK (STFC). This study was supported by the Finnish Academy of Science and Letters Vilho, Yrja and Kalle Vaisala Foundation (VP,VB), the Academy of Finland projects 115920 (AK) and 138775 (KK). We appreciate the constructive comments of both reviewers.

References

Alperovich, L.S., Fedorov, E.N., Volgin, A.V., Pilipenko, V.A., Pokhil'ko, S.N., 1991. Doppler sounding as tool for the study of MHD wave structure in the ionosphere. Journal of Atmospheric and Terrestrial Physics 53, 581–586.

Alperovich, L.S., Fedorov, E.N., 2007. Hydromagnetic Waves in the Magnetosphere and the Ionosphere. Series: Astrophysics and Space Science Library 353 (XXIV), 418 ISBN:978-1-4020-6636-8.

Belakhovsky, V.B., Pilipenko, V.A., 2011. Excitation of Pc5 pulsations of magnetic field and particle fluxes at the recovery phase of the magnetic storm 31.10.2003. Geomagnetism and Aeronomy 51, 608–629.

Clauer, C.R., Ridley, A.J., Sitar, R.J., Singer, H.J., Rodger, A.S., Friis-Cristensen, E., Papitashvili, V.A., 1997. Field line resonant pulsations associated with a strong dayside ionospheric shear convection flow reversal. Journal of Geophysical Research 102, 4585–4596.

Fedorov, E., Pilipenko, V., Surkov, V., Rao, D.R.K., Yumoto, K., 1999. Ionospheric propagation of magnetohydrodynamic disturbances from the equatorial electrojet. Journal of Geophysical Research 104, 4329–4336.

Fenrich, F.R., Waters, C.L., Connors, M., Bredeson, C., 2006. Ionospheric signatures of ULF waves: Passive radar techniques. In: Magnetospheric ULF Waves: Synthesis and New Directions, vol. 169. AGU Geophysical Monograph.

Georges, T.M., 1973. Infrasound from convective storms: examining the evidence. Reviews of Geophysics 11, 571.

Hughes, W.J., Southwood, D.J., 1976. The screening of micropulsation signals by the atmosphere and ionosphere. Journal of Geophysical Research 81, 3234–3240.

Ikeda, A., Yumoto, K., Uozumi, T., Shinohara, M., Nozaki, K., Yoshikawa, A., Bychkov, V.V., Shevtsov, B.M., 2010. Phase relation between Pi2-associated ionospheric Doppler velocity and magnetic pulsations observed at a mid-latitude MAGDAS station. Journal of Geophysical Research 115, A02215. doi:10.1029/2009JA014397.

Kivelson, M.G., Etcheto, J., Trotignon, J.G., 1984. Global compressional oscillations of the terrestrial magnetosphere: the evidence and a model. Journal of Geophysical Research 89, 9851.

Kleimenova, N.G., Kozyreva, O.V., 2005. Spatial-temporal dynamics of Pi3 and Pc5 geomagnetic pulsations during the extreme magnetic storms in October 2003. Geomagnetism and Aeronomy (English Translation) 45, 71–79.

Knudsen, D., Kelley, M., Vickrey, J., 1992. Alfvén waves in the auroral ionosphere: a numerical model compared with measurements. Journal of Geophysical Research 97, 77–90.

Leonovich, A.S., Kozlov, D.A., Pilipenko, V.A., 2006. Slow magnetosonic resonance in a dipole-like magnetosphere. Annales Geophysicae 24, 2277–2289.

Leonovich, A.S., Mazur, V.A., 2005. Why do ultra-low-frequency MHD oscillations with a discrete spectrum exist in the magnetosphere? Annales Geophysicae 23, 1075–1079.

Author's personal copy

Mann, I.R., Wright, A.N., Mills, K., Nakariakov, V.M., 1999. Excitation of magnetospheric waveguide modes by magnetosheath flows. Journal of Geophysical Research 104, 333.

Nenovski, P., 2001. Polarization effects of the finite-size low-altitude ionosphere. Space Science Reviews 95, 581–598.

Nishida, A., 1964. Ionospheric screening effect and storm sudden commencement. Journal of Geophysical Research 69, 1861.

Pilipenko, V., Fedorov, E., 1995. Modulation of total electron content in the ionosphere by geomagnetic pulsations. Geomagnetism and Aeronomy (English Translation) 34, 516–519.

Pilipenko, V., Vellante, M., Fedorov, E., 2000. Distortion of the ULF wave spatial structure upon transmission through the ionosphere. Journal of Geophysical Research 105, 21225–21236.

Pilipenko, V., Fedorov, E., Heilig, B., Engebretson, M.J., 2008. Structure of ULF Pc3 waves at low altitudes. Journal of Geophysical Research 113, A11208. doi:10.1029/2008JA013243.

Pilipenko, V., Kozyreva, O., Belakhovsky, V., Engebretson, M.J., Samsonov, S., 2010. Generation of magnetic and particle Pc5 pulsations at the recovery phase of strong magnetic storms. Proceedings of the Royal Society A. doi:10.1098/rspa.2010.0079.

Pilipenko, V., Fedorov, E., Heilig, B., Engebretson, M.J., Sutcliffe, P., Lühr, H., 2011. ULF waves in the topside ionosphere: satellite observations and modeling. In: Liu, William, Fujimoto, Masaki (Eds.), The Dynamic Magnetosphere, IAGA Special Sopron book series, vol. 3, Springer, pp. 257–269. doi:10.1007/978-94-007-0501-2.

Pogorel'zev, A.I., 1989. Electric and magnetic field disturbances induced by the atmospheric waves interaction with the ionospheric plasma. Geomagnetism and Aeronomy 29, 286–292.

Pokhotelov, O.A., Pilipenko, V.A., Amata, E., 1985. Drift-anisotropy instability of a finite-beta magnetospheric plasma. Planetary and Space Science 33, 1229–1241.

Poole, A.W.V., Sutcliffe, P.R., 1987. Mechanisms for observed total electron content pulsations at mid latitudes. Journal of Atmospheric and Terrestrial Physics 49, 231–236.

Potapov, A., Guglielmi, A., Tsegmed, B., Kultima, J., 2006. Global Pc5 event during 29–31 October 2003 magnetic storm. Advances in Space Research 38, 1582–1586.

Samson, J.C., Greenwald, R.A., Ruohoniemi, J.M., Hughes, T.J., Wallis, D.D., 1991. Magnetometer data and radar observations of MHD cavity modes in the Earth's magnetosphere. Canadian Journal of Physics 69, 929–937.

Sutcliffe, P.R., Poole, A.W.V., 1990. The relationship between ULF geomagnetic pulsations and ionospheric Doppler oscillations: model predictions. Planetary and Space Science 38, 1581–1589.

Sutcliffe, P.R., Luhr, H., 2005. A comparison of Pi2 pulsations observed by CHAMP in low Earth orbit and on the ground at low latitudes. Geophysical Research Letters 30. doi:10.1029/2003GL018270.

Walker, A.D.M., Greenwald, R.A., Stuart, W.F., Green, C.A., 1979. STARE auroral radar observations of Pc5 geomagnetic pulsations. Journal of Geophysical Research 84, 3373–3388.

Yagova, N., Pilipenko, V., Fedorov, E., Vellante, M., Yumoto, K., 1999. Influence of ionospheric conductivity on mid-latitude Pc3-4 pulsations. Earth, Planets and Space 51, 129–138.

Yeoman, T.K., Lester, M., Orr, D., Lühr, H., 1990. Ionospheric boundary conditions of hydromagnetic waves: the dependence on azimuthal wavenumber and a case study. Planetary and Space Science 38, 1315–1325.

Yeoman, T.K., Wright, D.M., Chapman, P.J., Stockton-Chalk, A.B., 2000. High-latitude observations of ULF waves with large azimuthal wavenumbers. Journal of Geophysical Research 105, 5453–5462.

Yoshikawa, A., Itonaga, M., 1996. Reflection of shear Alfven waves at the ionosphere and the divergent Hall current. Geophysical Research Letters 23, 101–104.

Yoshikawa, A., Obana, Y., Shinohara, M., Itonaga, M., Yumoto, K., 2002. Hall-induced inductive shielding effect on geomagnetic pulsations. Geophysical Research Letters 29, 8. doi:10.1029/2001GL013610.

Published by SERC of Kyushu University
I S W I
Newsletter
under the auspices of the United Nations

This pdf was circulated in Volume 4, Number 37, on 3 April 2012.